Physics of one-dimensional hybrids based on carbon nanotubes

Gao, Jia

Chapter 2

Encapsulation of conjugated oligomers in single-walled carbon nanotubes: towards nano-hybrids for photonic devices

In this chapter, we demonstrate a nano-hybrid with light emitting properties in the visible spectral range obtained by encapsulating thiophene oligomers in SWNTs. By Raman spectroscopy and high resolution transmission electron microscopy (HRTEM) we have revealed the endohedral position of the guest molecules. Surprisingly, these are not situated in a single array in the center of the tube but are instead arranged in two lines along the sidewalls. Density functional theory (DFT) including van der Waals interactions provides the maximal binding energy for the molecules in cofacial arrangement. The hybrids show photoluminescence in the visible range while a reduced lifetime of the excited state is symptomatic of molecule – SWNT electronic interactions. We suggest this class of supramolecular hybrid as a promising compact and robust source of photons for the next generation of photonic and optoelectronic devices.[*]

[*] M. A. Loi, J. Gao , F. Cordella, P. Blondeau, E. Menna, B. Bártová, C. Hébert, S. Lazar, G. A. Botton, M. Milko, C. Ambrosch-Draxl, *Adv. Mater*, **2010**, 22, 1635-1639.

2.1 Introduction

Building robust optoelectronic devices at the atomic scale is one of the challenges faced by nanotechnology. Single-walled carbon nanotubes (SWNTs) are extremely robust nano-objects that exhibit unique electron transport, but their small band gap limits them to be only near infrared emitters. [1, 2] In contrast, organic molecules having outstanding photophysical properties often suffer from low stability and poor electrical characteristics. Exploiting the advantages of both SWNTs and organic molecules opens the prospective to obtain fascinating systems with one-dimensional charge transport and light emission in the visible spectral range. A promising strategy to achieve this is to make use of the hollow space within SWNTs (so-called pods) to accommodate organic molecules (so-called peas) creating a new hybrid system. [3] Since the discovery in 1998 that the hollow space inside SWNT could be filled, various atoms and molecules have been encapsulated, including: fullerenes, fullerene derivatives, alkali metal and metallocenes. [4-7] Several experimental and theoretical investigations have shown that the physico-chemical properties of these new materials are strongly influenced by their specific interactions and their confinement in the one-dimensional cavity. [8-10] To date, few attempts [4-6] have been made to synthesize non-fullerene peapods. Kataura et al. [11] prepared composites with Zn-diphenylporphyrin pea, and more recently, Yanagi et al. [12] succeeded in encapsulating β-carotene molecules. However, photoluminescence has not yet been demonstrated for any peapods system.

Here, we report on nano-hybrids composed of SWNTs and α-sexithiophene (6T) (Figure 2.1) which were obtained following a procedure based on the sublimation of sexithiophene [13] in the presence of SWNTs of diameters between 1.2 and 1.5 nm in a sealed quartz tube at low pressure. Extensive washings of the resulting product were performed to remove exohedral molecules from the peapod sidewalls. Such hybrids will be referred to as 6T@SWNT.

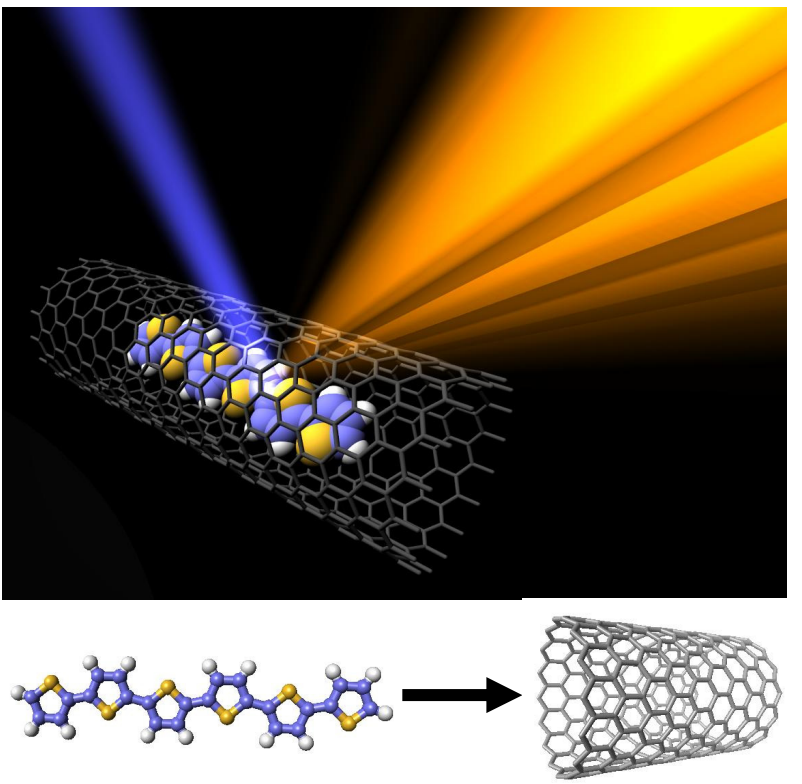

Figure 2.1 Nano-hybrids and their functionality. Top: cartoon of the visible light emitting 6T@SWNT peapod. Bottom: schematic of the encapsulation of α-sexithiophene in SWNTs. The yellow color indicates the sulfur, blue the carbon, and white the hydrogen.

2.2 Results and discussion

HRTEM images (Figure 2.2) taken with an aberration-corrected (Cs-corrected FEI Titan 80-300 Cubed) microscope reveal the successful encapsulation of 6T molecules inside SWNTs. Surprisingly, in most cases two almost parallel chains of 6T molecules are visible. They are accommodated along the sidewalls of the tube with a small tube-molecule distance in the range of 0.32-0.35 nm. In contrast, the spacing between the molecules varies from 0.4-0.8 nm, depending on the tube diameter. Image simulations based on a multislice approach [14, 15] give insight into the actual arrangement of the sexithiophene molecules inside the tubes. Figure 2.2(b) shows the images for two (perfectly straight) molecules in a parallel alignment inside a (15,0) SWNT with 1.18 nm diameter together with the

corresponding atomic models. For the cases where the electron beam is parallel (top) and perpendicular (bottom) to the molecular plane the images are depicted for different defocus varying from -4 to +4 nm in steps of 2 nm. Upon comparison with the measured images reported in Figure 2.2 we conclude that most of the molecules in our sample appear in an arrangement as given in Figure 2.2(a) aligning with respect to the electron beam. However, some twisting of the molecules as well as slight tilts between them might occur.

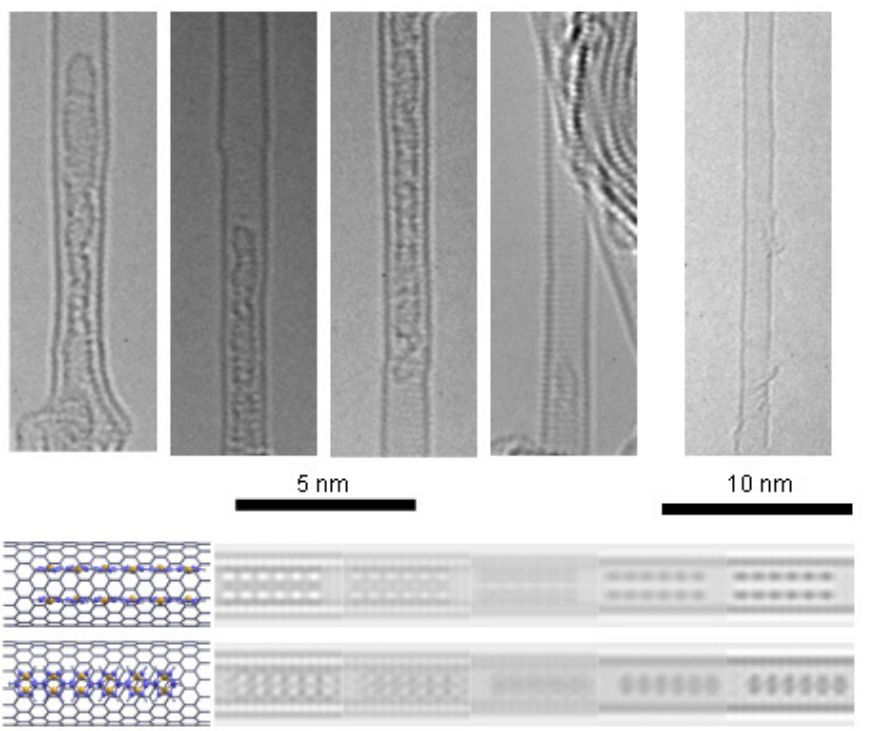

Figure 2.2 HRTEM images and simulations. (a) Measured TEM images of 6T@SWNT (four images on the left); pristine nanotube (right). (b) Atomic model of 6T molecules inside a (15,0) SWNT in two different projections (left) together with multi-slice simulations (right). The electron beam is assumed to be parallel (top) and perpendicular (bottom) to the molecular plane. The defocus varies between -4 to +4 nm in steps of 2 nm (from left to right).

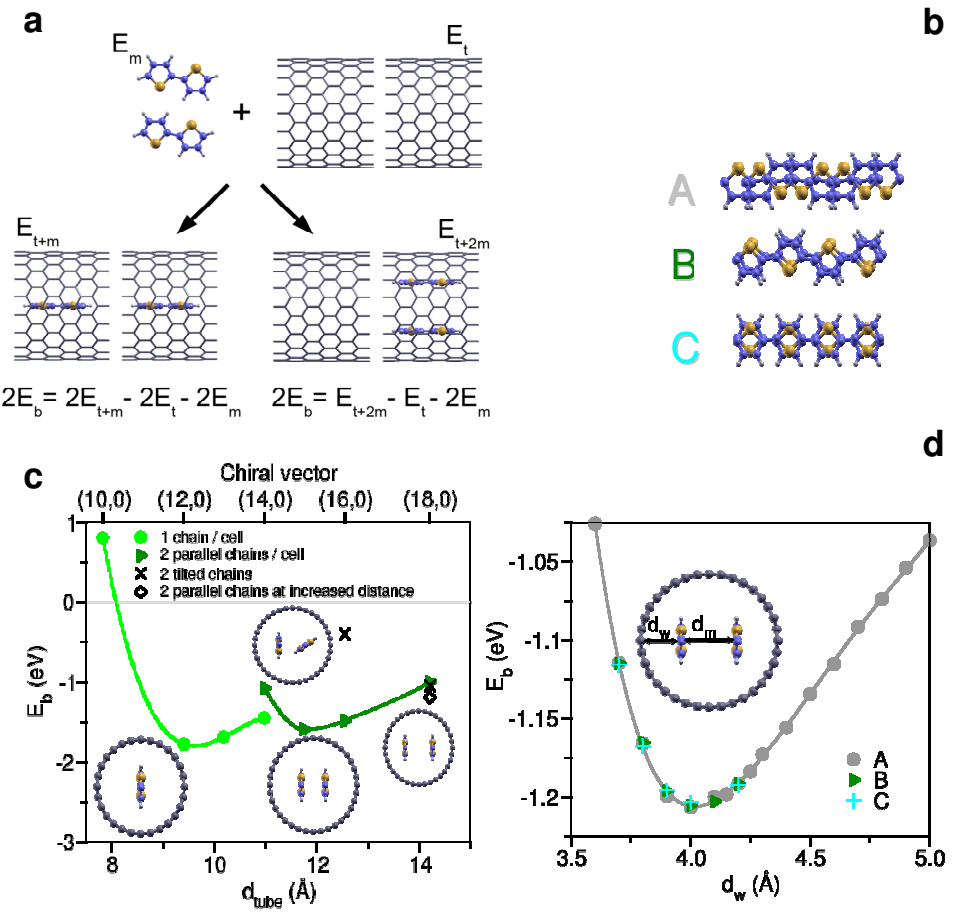

Figure 2.3 Calculated binding energy. (a) Schematic showing the possibilities for two molecules to be embedded in a SWNT and the corresponding binding energies. (b) Configurations, where two encapsulated chains are shifted with respect to each other by half (A), zero (B), and one thiophene ring (C), respectively. (c) Binding energy as a function of tube diameter for (n,0) peapods with one and two polythiophene chains encapsulated in the unit cell. For the latter, the two chains are considered at a fixed distance. The data point marked by the diamond is obtained for a larger interchain distance, while the crosses refer to tilted configurations. (d) Binding energy for two polythiophene chains encapsulated in an (18,0) SWNT as a function of the distance to the tube wall (d_w).

The stability of peapods was studied by total energy calculations for (n,0) nanotubes with either one or two polythiophene chains encapsulated. [16] For the latter case, we have first adopted an interchain distance d_m=3.9 Å found for two free-standing molecules in a parallel configuration. The binding energy, E_b, was obtained according to the two formulas shown in the schematic, Figure 2.3(a) where E_b is normalized to one molecule per repeat unit. Figure 2.3(c) gives clear evidence that embedding two molecules is favorable for tubes with diameter larger

than 1.1 nm (the range used in this work) while very small tubes allow the accommodation of only one chain per molecule. To find the actual arrangement of the thiophene molecules with respect to each other, we performed additional calculations with a tilted configuration marked by crosses. For small tubes this situation is not favorable, but for larger ones, the energy is less sensitive to the tilt angle. However, the binding energy increases by changing the interchain spacing as concluded from the data point indicated by the diamond. The corresponding energy dependence is depicted in more detail in Figure 2.3(d) showing that for an (18,0) SWNT the optimal distance of the polymer chain to the tube wall is roughly d_w=4 Å, distinctly smaller than the interchain distance of d_m=6.2 Å. Therefore, the van der Waals bond between the polymer and the tube turns out to be stronger than the intermolecular interaction. This also explains why the results are independent of the relative positions of the two chains, i.e., resulting in the same binding energy for configurations A, B, and C shown in Figure 2.3(d). In summary, the surprising features revealed by HRTEM are confirmed by theory, (i) the observation of two parallel molecules in the tubes, (ii) their preference to be located in the vicinity of the tube walls, as well as (iii) the fact that they appear shifted with respect to each other, thereby mimicking continuous chains observed experimentally.

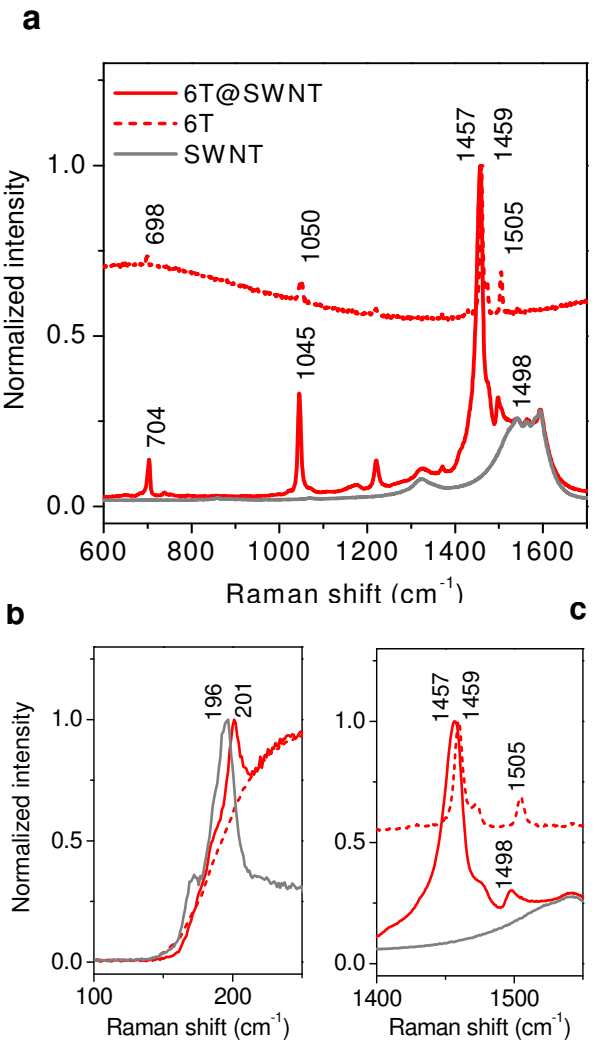

Figure 2.4 Raman spectroscopy. (a) Raman spectra of 6T@SWNT, 6T, and SWNTs excited at 633 nm. (b) Radial breathing mode (RBM) of 6T@SWNT and SWNTs. (c) C=C stretching modes of 6T@SWNT and 6T. All spectra are normalized with respect to their maximum peak frequencies.

The Raman spectra of the oligomer, the SWNTs and the 6T@SWNT excited at 633 nm are shown in Figure 2.4. After encapsulation, the radial breathing mode (RBM) of the SWNT is shifted up by about 5 cm^{-1}, as shown in Figure 2.4(b). Such shift can be ascribed to hardening and stiffening of C-C bonds [17] and is not present in the control experiment which was performed after mixing SWNTs and the 6T in a ratio 10:1. The frequency variation of the RBM is an unambiguous fingerprint of the

inclusion of peas in the hollow space of the SWNTs also reported for fullerene-based peapods. [11]

The most intense bands of the oligothiophenes are found in the spectral region between 600 and 1600 cm^{-1} [18-20] (Figure 2.4(a)) which are, in case of 6T, the C-S-C deformation (698 cm^{-1}), the C-H bending (1050 cm^{-1}), the C-C inter-ring stretching (1221 cm^{-1}), and the C=C stretching (1459 and 1505 cm^{-1}). For 6T@SWNT, some of them are shifted, e.g. from 698 to 704 cm^{-1} and from 1050 to 1045 cm^{-1} as well as from 1459 to 1457 cm^{-1}. Moreover, a new peak appears at 1498 cm^{-1} (Figure 2.4(c)).

Raman measurements also allow determining a possible charge transfer between the oligomer and the SWNT. In fact, the radical cation ($6T^{+}$) has been evidenced to give rise to a large change of the C-C stretching from 1459 to 1440 cm^{-1}. [21] Besides that, a charge transfer between the encapsulated molecules and the SWNT has been reported to cause a shift of the G-band and a RBM intensity reduction. [4, 22] Here, none of these effects could be observed, suggesting that charge transfer is not occurring, a fact which is supported by our DFT calculations.

For achieving tunable light emitting nano-hybrids, the question is how the SWNT affects the emission properties of the encapsulated oligothiophene molecules.

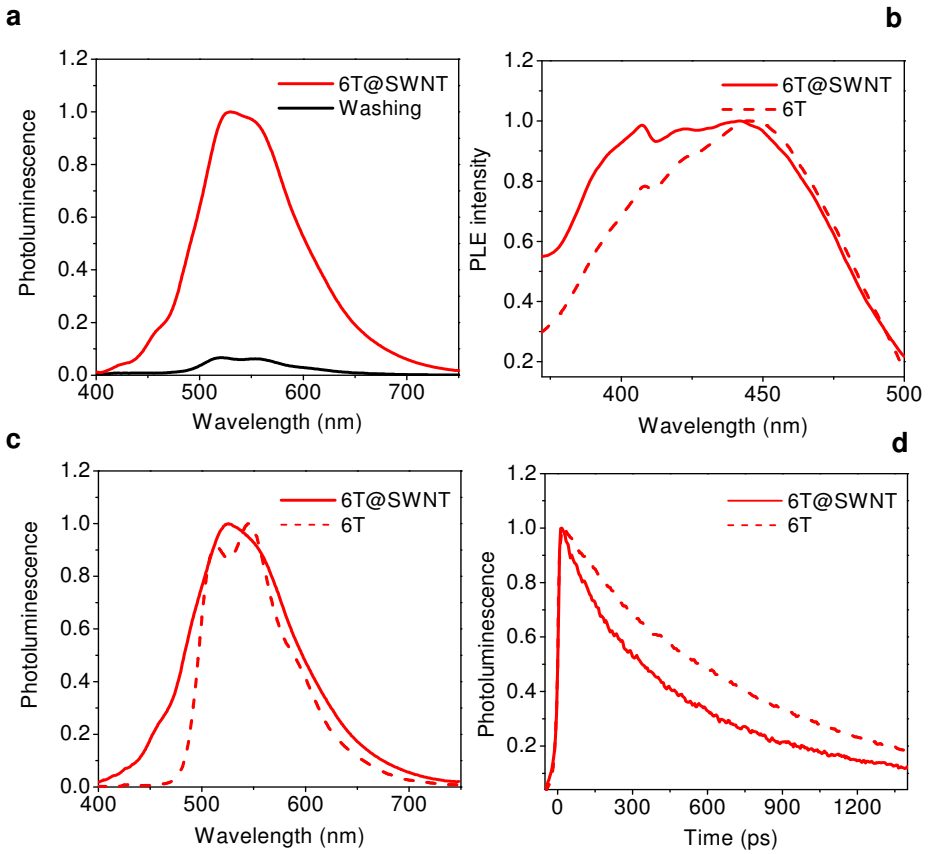

Figure 2.5 Optical spectroscopy. (a) Photoluminescence spectra of 6T@SWNT and of the washing solution after 18 hours of washing. (b) Photoluminescence excitation spectra of 6T@SWNT and of 6T in solution detected at 550 nm. (c) Photoluminescence spectra of 6T and 6T@SWNT. (d) PL decays of 6T@SWNT and 6T at 515 nm. The excitation wavelength for all PL measurements is 380 nm.

In Figure 2.5 the photoluminescence excitation and photoluminescence spectra of 6T@SWNT are reported in comparison with the corresponding spectra of the 6T molecule and the SWNTs in dimethylformamide (DMF) solution. In the absorption spectra the main feature of encapsulated 6T appears to be red-shifted compared to the one of the isolated molecules in solution. [23] A comparable red-shift has been reported previously for similar systems [24] and it is rationalized with the interaction of the 6T molecules with the SWNT walls. However, the different post-synthetic processes used to obtain the peapods solution make the comparison of the absorption spectra not completely reliable. In fact, a lower degree of SWNTs bundles in the peapods samples can change the nanotube absorption shape determining the apparent red-shift of the 6T signature. The photoluminescence

excitation (PLE) can give a more precise idea of the absorbing states. In Figure 2.5(b) is reported the PLE spectrum of the 6T@SWNT compared with the one of 6T in solution both spectra detected at 550 nm. The two spectra show that the main feature is almost super-imposed while the high energy part of the peapod spectrum is more pronounced with respect to that of the molecules in solution indicating a possible energy transfer from higher excited states of the SWNTs to the encapsulated 6T molecules.

The PL emission of the hybrid compared to that of 6T in solution shows broader and less resolved features (Figure 2.5(a) and 2.5(c)). Being extremely sensitive to supra-molecular interactions, [25] the PL spectra allow for the recognition of different relative arrangements of molecules. In this case the interaction between 6T molecules inside the SWNT does not appear to be important. Moreover, in view of the findings of theory, TEM and Raman experiments we can state that the interaction of the 6T molecule with the tube walls is dominant. In fact, the intermolecular distances found theoretically as well as by HRTEM rule out the interaction between the paired molecules in favor of the interaction between the molecules and the side walls of the tube. Here we stress the rather efficient emission of the peapods in the visible spectral range in contrast to previously reported results showing complete PL quenching. [24, 26] It is important to underline that 6T@SWNT has been extensively washed to remove exohedral molecules. The effectiveness of the washing procedure is proven by the negligible PL emission of the last washing solution shown in Figure 2.5(a).

Time-resolved measurements (Figure 2.5(d)) show a shorter PL lifetime of the peapod being 563 ps, compared to that of the 6T molecule in the same solvent (τ = 813 ps). Also in this case, the explanation of the faster PL decay can be found in the quenching by the SWNT cage. The SWNTs used for the peapods synthesis are composed of both semiconducting and metallic tubes. It has been proven that the excited state lifetime of isolated SWNTs in the range of tens to hundreds of a picosecond is dominated by nonradiative processes. Consequently, for SWNT bundles the PL quenching caused by the metallic nanotubes reaches the femto-second range. [27] This effect can provide an additional nonradiative path for the encapsulated molecule. Moreover, Förster energy transfer from the 6T molecule to the SWNT should also be considered as a possible explanation. As already discussed, charge transfer between the encapsulated molecules and the SWNT appears to be unlikely.

DFT calculations reveal the binding of the pea and pod to be of van der Waals character. This fact is also highlighted in the electronic structure where the bands of the peapod appear like a mere superposition of those stemming from the two subsystems. Therefore, one can expect the optical spectra to generally exhibit the same features as those of the pea plus the pod, with the actual peak positions

determined by the alignment of the molecular levels with the SWNT bands. A possible explanation for the shorter decay time could be found in weak additional transitions between the pea and the pod, which could alter the nature and size of excitons and hence provide new decay channels.

2.3 Conclusions

In summary, we have successfully synthesized peapods combining rigid-rod like molecules with SWNTs. HRTEM and optical probes show evidence of the encapsulation, density functional calculations confirm the experimental findings and provide deeper insight concerning stability and electronic properties of these systems. We demonstrate that such nano-hybrids, emitting light in the visible range of the spectrum, are a promising photon sources to be used in future opto-electronic devices.

2.4 Experimental details

Sample preparation instruments
For low power sonications a 150 W ultrasonic cleaning bath, operating at 45 kHz, was used, while for high power sonications a 600 W ultrasonic processor equipped with a titanium microtip was employed. A centrifuge IEC CL10 (Thermo) was utilized for all procedures. Solvents were purchased from Sigma-Aldrich and oligothiophenes from TCI.

Purification of SWNTs
SWNTs from Nanocarblab (arc-discharge, 80% purity) were annealed at 1100 °C under vacuum (10^{-6} Torr).

Encapsulation of oligothiophenes
A suspension of SWNTs (5 mg) in toluene (1 mL) was sonicated at high power for 10 min. Then the oligothiophenes (5 mg) were added and the solvent was evaporated. The resulting solid mixture was placed in a sealed quartz tube at reduced pressure (P = 10^{-3} Torr) and heated for 3 days (T=320 °C). The mixture was sonicated at low power for 10 min in toluene (15 mL), then centrifugated (10 min, 4k rpm), and the supernatant phase removed. This washing procedure was repeated at least 30 times in order to remove exohedral molecules. The concentration of oligothiophene in the supernatant phase was checked by PL spectroscopy showing a negligible 6T content in the last washing. The solid residue was dried under N_2 flow.

Control experiments were performed using the following procedure: A suspension of SWNTs (1 mg) in CH_2Cl_2 (1 mL) was sonicated at high power for 10 min, then added to a solution of the oligothiophene (0.1 mg) in CH_2Cl_2 (1 mL), and the solvent was quickly evaporated under N_2 flow in order to avoid any encapsulation.

HRTEM

For the HRTEM measurements a suspension of 6T@SWNT in toluene was sonicated for 10 min and dropped onto a holey carbon grid. A FEI Titan 80-300 Cubed high-resolution transmission electron microscope equipped with a CEOS-designed hexapole-based aberration corrector for the image-forming lens was operated at 80 kV. Therefore the electron knock-on damage to the sample was reduced. The instrument is fitted with a Super-Twin lens in order to achieve sub-Ångstrom resolution for phase contrast imaging. The specimen was kept at room temperature during the experiment. The Gatan US1000 CCD camera was used for digital recording of HR-TEM pictures. The Cs was set to 2 µm and HRTEM focal series were recorded. We present the images with slightly under-focused conditions in order to enhance the contrast of the molecule inside the SWNT. The HRTEM image simulations were performed with a standard multislice procedure.

Theory

All calculations were performed in the framework of DFT utilizing the planewave code QUANTUM ESPRESSO. A super-cell approach was adopted with twice the repeat unit of the SWNT along the tube axis, and a large enough vacuum size of 8 Å perpendicular to it to prevent interactions of neighboring unit cells. In a first step, the structures were optimized for both, the SWNT and the polymer independently, employing the generalized gradient approximation (GGA), and using 4 k points in the irreducible wedge of the Brillouin zone. The systems were considered to be relaxed when all atomic forces were smaller than 1 mRy / Å. These geometries were taken as a starting point for the investigations of the combined systems. To ensure commensurability of the polymer with the SWNT, the former had to be stretched by 8%. The energies of all configurations were calculated by treating the van der Waals interactions in an ab-initio manner.

Optical spectroscopy

UV/Vis/NIR spectra were recorded with a Cary 5 Varian spectrometer. Raman spectra were performed with an Invia Renishaw Raman microspectrometer (50 objective) using a 488 nm and 633 nm laser lines of an Ar and He-Ne lasers at room temperature with a low laser power. The measurements were carried out with the samples on KBr discs.

For time resolved and steady state PL measurements the solutions were excited by a 150 fs pulsed Kerr mode locked Ti-sapphire laser, frequency doubled at about 380 nm and the steady PL emission was measured with CCD detector. The time-resolved PL was recorded by a Hamamatsu streak camera working in synchroscan mode. The decays were fitted using a single exponential decay function.
The photoluminescence excitation spectra (PLE) were recorded with a Perkin Elmer LS 50B spectrometer and detected at 550 nm. All measurements were performed at room temperature.

References

[1] J. A. Misewich, R. Martel, P. Avouris, J. C. Tsang, S. Heinze, J. Tersoff, *Science* **2003**, *300*, 783-786.
[2] J. Chen, V. Perebeinos, M. Freitag, J. Tsang, Q. Fu, J. Liu, P. Avouris, *Science* **2005**, *310*, 1171-1174.
[3] O. Vostrowsky, A. Hirsch, *Angew. Chem. Int. Ed.* **2004**, *43*, 2326-2329.
[4] T. Takenobu, T. Takano, M. Shiraishi, Y. Murakami, M. Ata, H. Kataura, Y. Achiba, Y. Iwasa, *Nat. Mater.* **2003**, *2*, 683-688.
[5] L. J. Li, A. N. Khlobystov, J. G. Wiltshire, G. A. D. Briggs, R. J. Nicholas, *Nat. Mater.* **2005**, *4*, 481-485.
[6] Y. Fujita, S. Bandow, S. Iijima, *Chem. Phys. Lett.* **2005**, *413*, 410-414.
[7] M. Monthioux, *Carbon* **2002**, *40*, 1809-1823.
[8] D. J. Hornbaker, S. J. Kahng, S. Misra, B. W. Smith, A. T. Johnson, E. J. Mele, D. E. Luzzi, A. Yazdani, *Science* **2002**, *295*, 828-831.
[9] A. N. Khlobystov, D. A. Britz, A. Ardavan, G. A. D. Briggs, *Phys. Rev. Lett.* **2004**, *92*, 245507.
[10] S. Campestrini, C. Corvaja, M. D. Nardi, C. Ducati, L. Franco, M. Maggini, M. Meneghetti, E. Menna, G. Ruaro, *Small* **2008**, *4*, 350-356.
[11] H. Kataura, Y. Maniwa, M. Abe, A. Fujiwara, T. Kodama, K. Kikuchi, H. Imahori, Y. Misaki, S. Suzuki, Y. Achiba, *Appl. Phys. A-Mater. Sci. Process.* **2002**, *74*, 349-354.
[12] K. Yanagi, Y. Miyata, H. Kataura, *Adv. Mater.* **2006**, *18*, 437-441.
[13] H. Kataura, Y. Maniwa, T. Kodama, K. Kikuchi, K. Hirahara, K. Suenaga, S. Iijima, S. Suzuki, Y. Achiba, W. Kratschmer, *Synth. Met.* **2001**, *121*, 1195-1196.
[14] P. A. Stadelmann, *Ultramicroscopy* **1987**, *21*, 131-145.
[15] P. A. Stadelmann, java EMS (JEMS), ver. 3.3518U2008; EPFL, Lausanne.
[16] For computational reasons, we have used polythiophene rather than 6T. This is well justified for such considerations as the polymer can be regarded as the limiting case of long oligomers
[17] D. A. Britz, A. N. Khlobystov, *Chem. Soc. Rev.* **2006**, *35*, 637-659.
[18] A. Degli Esposti, M. Fanti, M. Muccini, C. Taliani, G. Ruani, *J. Chem. Phys.* **2000**, *112*, 5957-5969.
[19] E. Agosti, M. Rivola, V. Hernandez, M. Del Zoppo, G. Zerbi, *Synth. Met.* **1999**, *100*, 101-112.
[20] G. Louarn, J. P. Buisson, S. Lefrant, D. Fichou, *J. Phys. Chem.* **1995**, *99*, 11399-11404.
[21] N. Yokonuma, Y. Furukawa, M. Tasumi, M. Kuroda, J. Nakayama, *Chem.*

Phys. Lett. **1996**, *255*, 431-436.
[22] L. Kavan, P. Rapta, L. Dunsch, M. J. Bronikowski, P. Willis, R. E. Smalley, *J. Phys. Chem. B* **2001**, *105*, 10764-10771.
[23] R. S. Becker, J. S. deMelo, A. L. Macanita, F. Elisei, *J. Phys. Chem*. **1996**, *100*, 18683-18695.
[24] K. Yanagi, K. Iakoubovskii, S. Kazaoui, N. Minami, Y. Maniwa, Y. Miyata, H. Kataura, *Phys. Rev. B* **2006**, *74*, 155420.
[25] E. Da Como, M. A. Loi, M. Murgia, R. Zamboni, M. Muccini, *J. Am. Chem. Soc.* **2006**, *128*, 4277-4281.
[26] K. Yanagi, K. Iakoubovskii, H. Matsui, H. Matsuzaki, H. Okamoto, Y. Miyata, Y. Maniwa, S. Kazaoui, N. Minami, H. Kataura, *J. Am. Chem. Soc*. **2007**, *129*, 4992-4997.
[27] L. J. Carlson, T. D. Krauss, *Acc. Chem. Res*. **2008**, *41*, 235-243.